

# Grain-size dependence of intergranular magnetic correlations in nanostructured metals

Jörg F. Löffler,<sup>a,b\*</sup> Werner Wagner<sup>a</sup> and Gernot Kosterz<sup>c</sup>

<sup>a</sup>Paul Scherrer Institut, CH-5232 Villigen PSI, Switzerland

<sup>b</sup>California Institute of Technology, W. M. Keck Laboratory, Pasadena, California 91125, USA

<sup>c</sup>ETH Zürich, Institut für Angewandte Physik, CH-8093 Zürich, Switzerland

Email: [loeffler@caltech.edu](mailto:loeffler@caltech.edu)

Magnetic small-angle neutron scattering experiments were performed on nanostructured Fe, Co and Ni samples of varying grain size, produced by inert-gas condensation. The experiments show that the spontaneous spatial magnetic correlations forming in zero-field extend over many individual grains. These correlations depend strongly on grain size. In Fe, they have a minimum at a grain size of around 35 nm and increase sharply for smaller grain sizes. The crossover occurs at grain sizes comparable with  $L_{\text{crit}} = \pi \delta$ , where  $\delta$  is the bulk domain-wall width. For grain sizes below  $L_{\text{crit}}$ , the results are explained on the basis of the random-anisotropy model, which takes into account that the magnetic alignment between the grains competes with the anisotropies of the individual grains. Above  $L_{\text{crit}}$ , where domain walls can form within one grain, the magnetization direction corresponds to the anisotropy direction varying from grain to grain, and the magnetic correlation length increases approximately linearly with grain size. Furthermore, the measurements on Fe, Co and Ni show that the spatial magnetic correlations measured by SANS are always larger than  $L_{\text{crit}}$ . This is in agreement with results of theoretical studies showing that nonuniform magnetization configurations can only exist in grains with sizes  $D > L_{\text{crit}}$ .

## 1. Introduction

Nanostructured materials, *i.e.* materials with grain sizes in the nanometer range, often reveal significant differences in their properties if compared with the coarse-grained bulk material. This holds in particular for magnetic nanostructured materials, where the grain size becomes comparable to the width of a domain wall.

Large ferromagnetic particles contain several domains. Thus, the magnetization reversal is determined by domain-wall motion, a mechanism which is relatively unimpeded by imperfections and leads to low coercive fields. In nanostructured materials, however, the grain size is far smaller than the size of a usual domain and becomes comparable to the width of a domain wall. When nanoparticles are consolidated into a solid nanostructured material, not only the grain size but also the exchange interaction between the grains influences markedly the macroscopic magnetic properties. In this solid, as opposed to isolated particles, the magnetic correlation is not necessarily confined to only one grain, but can extend over many individual grains. Small-angle neutron scattering (SANS) performed on these materials provides the opportunity to study both compositional and magnetic correlations simultaneously.

The influence of exchange interaction between different grains decreases with increasing grain size. Thus, we expect the magnetic correlation length to be strongly grain-size dependent. Indeed, magnetic measurements have shown that the coercivity of nano-

structured materials passes through a maximum at grain sizes comparable to the bulk domain-wall width (Herzer, 1992; Löffler *et al.*, 1998).

Furthermore, knowledge of the magnetic correlation length as a function of the grain size is important for several applications. For the development of ultra-high storage density in magnetic recording media, it is crucial to know to what extent the independence of individual particles can be maintained in the presence of interparticle coupling. Furthermore, recently developed nanocrystalline alloys like FINEMET (Yoshizawa *et al.*, 1988) are examples of materials with unique soft-magnetic properties, a consequence of their large inter-grain coupling and small grain size.

The relevant correlations determining the macroscopic magnetic properties such as remanence and coercivity occur on length scales of the order of the size of the grains. Thus, we performed magnetic SANS experiments on nanostructured Fe, Co and Ni samples with different grain sizes to measure directly the spatial extensions of the magnetic correlations in relation to the grain size.

## 2. Experimental procedure

The nanostructured samples were produced by the inert-gas condensation technique (Gleiter, 1989), *i.e.*, by evaporation of the raw material and condensation in He atmosphere, followed by consolidation by pressing. This produces solid disk-shaped samples with a diameter of 8 mm, thickness of 100–300  $\mu\text{m}$ , and grain size in the material of around 10 nm. By thermal annealing, the grain size was increased incrementally up to 100 nm.

The SANS measurements were carried out at the instrument V4 at the Hahn-Meitner-Institut, Berlin, using a neutron wavelength of  $\lambda = 8 \text{ \AA}$  with a wavelength spread of 10% FWHM ( $\Delta\lambda/\lambda = 0.1$ ). By using sample-to-detector (SD) positions between 1.2 m and 16 m, the  $Q$  range covered was  $0.02 \text{ nm}^{-1} < Q < 1.5 \text{ nm}^{-1}$  ( $Q = 4\pi \sin\theta/\lambda$ , with  $\theta = \text{half the scattering angle}$ ). In some cases  $Q_{\text{max}}$  was increased to  $2.3 \text{ nm}^{-1}$  by lifting the detector. One measurement sequence was performed at the D11 instrument of ILL Grenoble, which provided the possibility to measure at a distance of 36 m (corresponding to  $Q_{\text{min}} = 0.01 \text{ nm}^{-1}$ ) with a sufficiently high neutron flux.

The measurements were performed at room temperature. The specimens were placed between the pole pieces of an electromagnet, which allowed a homogeneous field of up to 10 kOe to be applied. The field was applied horizontally, perpendicular to the incoming neutron beam and parallel to the flat surfaces of the nanostructured samples. By correcting the intensity data and normalizing them to the incoherent scattering of a water sample, the microscopic differential scattering cross section  $d\sigma/d\Omega(Q)$  in units of barn/(sr. at.) was computed.

## 3. Scattering of an arrangement of (magnetic) particles with different sizes

In the SANS experiment, the neutrons monitor the spatial variations of both, the nuclear and magnetic scattering length densities. For an unpolarized neutron beam, the differential scattering cross section can be described by the sum of the magnetic and nuclear cross section terms,

$$\frac{d\sigma}{d\Omega} = \frac{d\sigma_{\text{mag}}}{d\Omega}(Q) + \frac{d\sigma_{\text{nuc}}}{d\Omega}(Q),$$

*i.e.*,

$$\frac{d\sigma}{d\Omega} = \frac{1}{N} D_{\text{mag}}^2 |\mathbf{M}(\mathbf{Q})|^2 \sin^2 \alpha + \frac{1}{N} |F(\mathbf{Q})|^2, \quad (1)$$

with  $\mathbf{M}(\mathbf{Q}) = \int d^3r \exp(i\mathbf{Q} \cdot \mathbf{r}) \mathbf{M}(\mathbf{r})$ , where the magnetization density  $\mathbf{M}(\mathbf{r})$  is given in units of Bohr magnetons ( $\mu_B$ ) per unit volume and  $D_{\text{mag}}^2 = 0.0729 \times 10^{-24} \text{ cm}^2 = 0.0729 \text{ barn}$ . The magnetic scattering follows a  $\sin^2 \alpha$  behavior, with  $\alpha$  the angle between the scattering vector  $\mathbf{Q}$  and the magnetization vector  $\mathbf{M}$ ;  $F(\mathbf{Q}) = \int d^3r \exp(i\mathbf{Q} \cdot \mathbf{r}) \rho(\mathbf{r})$ , with  $\rho(\mathbf{r})$  the scattering length density and  $N$  is the number of scatterers.

For an arrangement of spherically symmetric (magnetic) particles with different sizes (neglecting interparticle interference), the scattering cross section becomes

$$\frac{d\sigma}{d\Omega} = (\Delta b_{\text{mag}})^2 \sin^2 \alpha i_{\text{mag}}(Q, R) + (\Delta b_{\text{nuc}})^2 i_{\text{nuc}}(Q, R), \quad (2)$$

where  $i_{\text{mag}}$  and  $i_{\text{nuc}}$  are the structure functions of the phases generating the magnetic and the compositional (nuclear) contrast;  $\Delta b_{\text{mag}} = D_{\text{mag}} M(\mathbf{r})$  and  $\Delta b_{\text{nuc}} = \Omega \rho(\mathbf{r})$  are the magnetic and nuclear scattering lengths;  $\Omega$  is the atomic volume and  $M$  is the magnetization of the particle in units of Bohr magnetons. The structure function has the form

$$i(Q, R) = \frac{1}{\Omega} \int_R F_p^2(Q, R) V_p(R) N(R) dR. \quad (3)$$

Here,  $F_p(Q, R)$  is the particle form factor,  $V_p(R)$  is the volume of the particle at position  $R$  and  $N(R)dR$  is the incremental volume fraction of particles in the size interval between  $R$  and  $R + dR$ .

#### 4. Experimental results

Fig. 1 shows examples of SANS intensity contours, *i.e.* lines of equal intensity, on the two-dimensional SANS detector positioned at 16 m. The data were recorded from an as-prepared Fe sample having an average grain size of 12 nm, positioned in zero-field and in an external field of 10 kOe. Without external field the scattering pattern is isotropic, indicating random magnetic orientations which follow the random crystallographic orientations of the grains. The average over all directions  $\langle \sin^2 \alpha \rangle$  yields a factor of 2/3 (Shull & Wilkinson, 1955).

Forcing the magnetic moments to a common alignment by applying a sufficiently strong external field, the magnetic scattering is zero in the  $\mathbf{Q}$ -direction parallel to  $\mathbf{H}$  ( $\alpha = 0$ ), and follows the  $\sin^2 \alpha$  law for other directions [equation (1)]. This leads to an anisotropic scattering on the two-dimensional detector (cf. Fig. 1), where the scattering parallel to the external field is purely nuclear (representing the density structure) and the scattering perpendicular to the field is the sum of the nuclear and magnetic scattering.

Fig. 2 shows the scattering cross section after averaging the scattering data with regard to the angle  $\alpha$  (in the following denoted as 'radial scattering cross section') for as-prepared Fe, Co and Ni, measured in zero-field and in the maximum field of 10 kOe. For large  $Q$  values, the radial scattering curves measured with and without

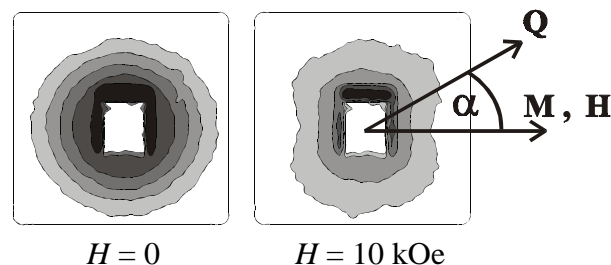


**Figure 1**  
Typical lines of equal SANS intensity on a two-dimensional detector from a nanostructured Fe sample for measurements in zero-magnetic field (left) and in a saturating external magnetic field  $H$  of 10 kOe (right), applied in horizontal direction ( $0.02 \text{ nm}^{-1} < Q < 0.16 \text{ nm}^{-1}$ ).

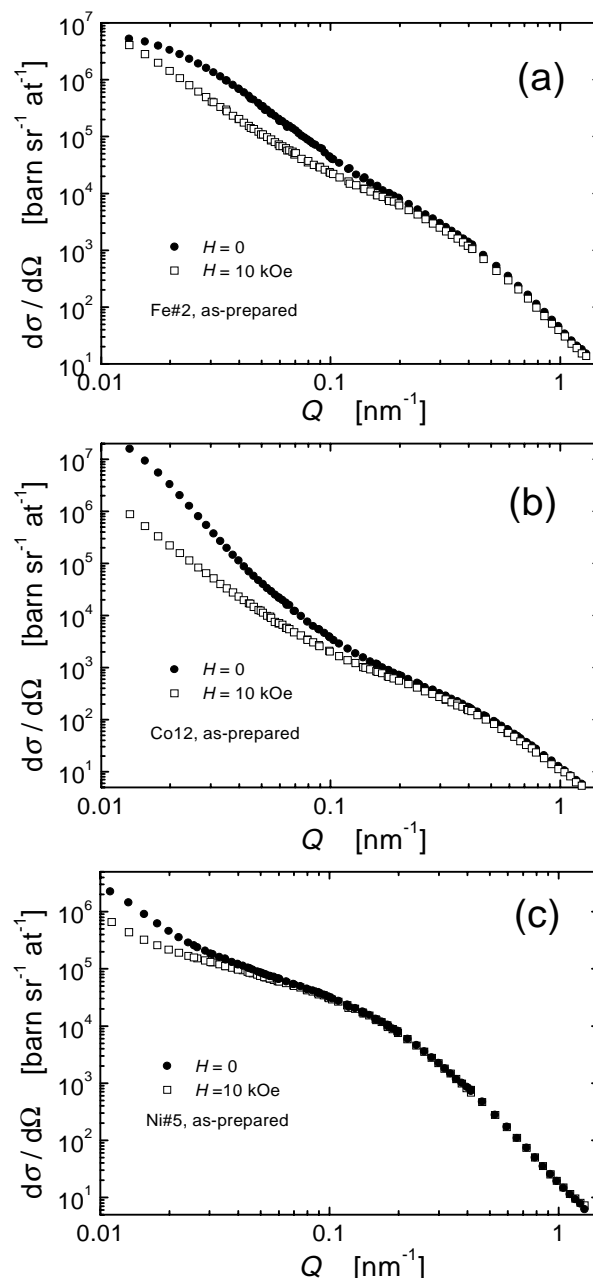


**Figure 2**  
Radial scattering cross section for as-prepared nanostructured Fe (a), Co (b) and Ni (c), measured at  $H = 0$  and  $H = 10 \text{ kOe}$ .

magnetic field lie closely together and are parallel for all three materials; for smaller  $Q$  a significant splitting is observed which is due to an extra magnetic scattering in zero-field. These  $Q$  values, where this extra scattering occurs, correspond to correlation lengths considerably larger than the grain size of 12 nm. Therefore, the results give evidence that spontaneous magnetic correlations forming at  $H = 0$  extend over several grains, as found already in earlier SANS studies (Wagner *et al.*, 1991; Wagner *et al.*, 1995; Löffler *et al.*, 1997; Weissmüller *et al.*, 1997). The present SANS study involving the three elements Fe, Ni and Co with quite different anisotropies reveals a systematic decrease of the correlation length with increasing anisotropy constant in the as-prepared samples. More specifically, we observe that the splitting of the SANS intensity profiles occurs at the highest  $Q$  value for Co and shifts progressively to lower values for Fe and Ni (cf. Fig. 2).

For a quantitative analysis of the SANS data, we followed a data evaluation proposed by Wagner *et al.* (1991). We assume that, in an external field of 10 kOe, the forced common magnetic alignment extends to such large distances that it can no longer be resolved by SANS. In this case, the scattering arises from an isotropic, nuclear scattering of grains embedded in a (diluted) interfacial phase, superimposed on an anisotropic, magnetic scattering of grains contrasted against an interfacial phase of different magnetic moment. The latter has its maximum perpendicular to the external field direction. In zero-field, where the magnetic scattering is also isotropic, a third contribution is superimposed, which is the contribution of magnetically correlated grains.

Within our model, in an external field of 10 kOe, the magnetization vector of all grains is fixed in the direction of the external field; thus, the average of  $\sin^2\alpha$  yields 1/2. Using equation (2), the differential scattering cross section then becomes

$$\frac{d\sigma}{d\Omega} = \left( \frac{1}{2} (\Delta b_{\text{mag}})^2 + (\Delta b_{\text{nuc}})^2 \right) i_p(Q, R), \quad (4)$$

with  $i_p$  the structure function of the particles, cf. equation (3). In zero-magnetic field,

$$\frac{d\sigma}{d\Omega} = \left( \frac{2}{3} (\Delta b_{\text{mag}})^2 + (\Delta b_{\text{nuc}})^2 \right) i_p(Q, R) + \frac{2}{3} (\Delta b_{\text{mag}})^2 i_{\text{corr}}(Q, R_{\text{corr}}), \quad (5)$$

with  $i_{\text{corr}}$  the structure function, and  $R_{\text{corr}}$  the radius, of the intergranular magnetic correlations.

Using equation (4) and the measurements at 10 kOe, we obtain the grain size distribution of our samples. To parameterize  $N(R)$  in equation (3), we chose a log-normal distribution, following TEM investigations (Haas & Birringer, 1992) revealing a log-normal distribution of the nanometer sized grains, *i.e.*,

$$N(R_i) = B \exp \left( - \frac{(\log(R_i / R_0))^2}{2\sigma^2} \right), \quad (6)$$

with  $B$  the amplitude,  $\sigma$  the width and  $R_0$  the position of the log-normal distribution. We assumed spherical particles to calculate  $F_p(Q, R)$  and  $V_p(R)$  in equation (3). The (volume-weighted) average grain size  $D (= 2R)$  obtained from our SANS measurements agrees well with the average grain size obtained from x-ray diffraction from an evaluation of the integral breadths of the Bragg peaks by the method of Klug & Alexander (1974). This agreement provides

further support for our assumption that at 10 kOe predominantly the nuclear and magnetic scattering of grains is observed.

More interestingly, we can extract the intergranular magnetic correlation distances by subtracting the scattering at 10 kOe from the scattering measured in zero-field, cf. equations (4) and (5). For several Fe samples, Fig. 3 shows the difference between the radial scattering cross section measured in zero-field and the radial scattering cross section measured at 10 kOe, in the following denoted as 'difference scattering curve'. The solid lines in Fig. 3 represent fits to the data according to equations (3) to (6), assuming spherical correlation volumes  $V_{\text{corr}}(R)$ . The difference curves of the samples with large grain sizes show slopes steeper than the exponent of -4 in the log-log plot (Fig. 3b). Such exponents are not explained by the kinematic scattering theory and can therefore not be fitted. It is likely that the magnetic correlations in these samples are so large that they can no longer be resolved by SANS. On the other hand, with increasing domain size, refraction effects play a progressively dominating role. Multiple refraction effects, which cause a broadening of the primary neutron beam, are known to occur from coarse-grained ferromagnetic materials with large domain sizes (see, e.g., Kosterz, 1979). Beyond a grain size of 80 nm our data evaluation is therefore no longer reliable. However, when the samples show effects of multiple refraction, we presume that they have magnetic correlations much larger than 150 nm.

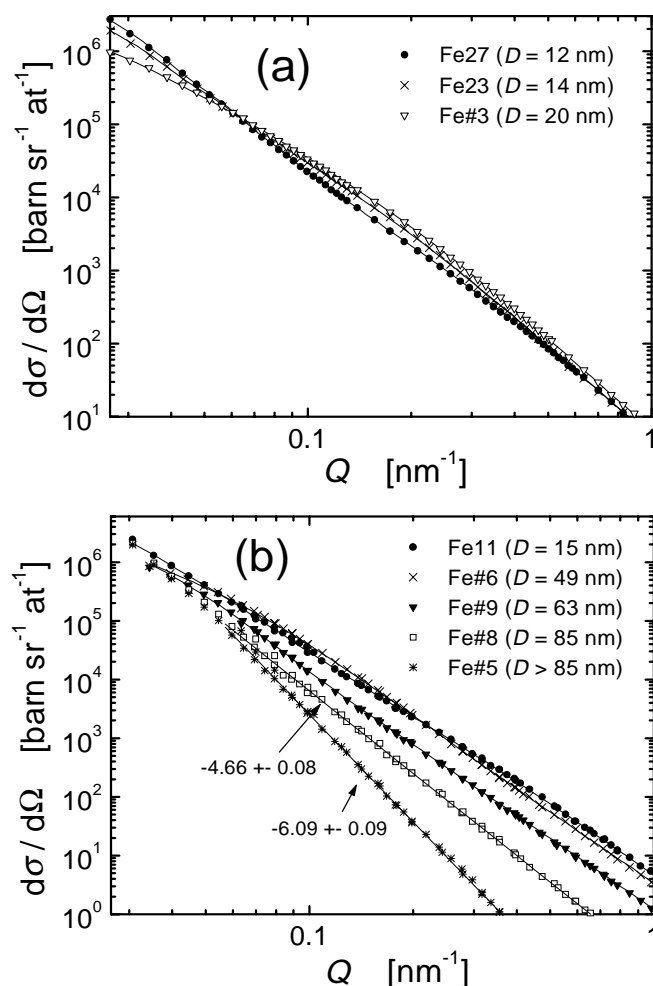


**Figure 3**  
Difference scattering curves of Fe samples with different grain sizes (values given in parentheses). The solid lines represent fits to the data as described in the text.

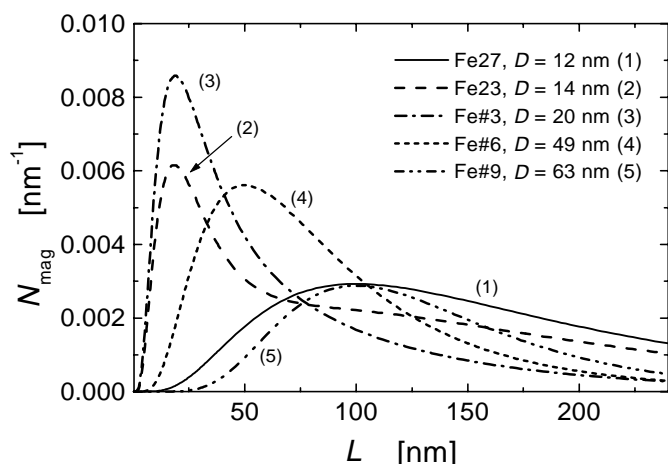


**Figure 4**

Size distribution  $N_{\text{mag}}$  of the spatial magnetic correlations, calculated from the SANS data of the Fe samples of Fig. 3. The numbers (1) to (5) represent the sequence of grain size in increasing order.

Fig. 4 shows the size distribution  $N_{\text{mag}}(L = 2R_{\text{corr}})$  of the spatial magnetic correlations calculated from the fits of Fig. 3. The curves are numbered (1) to (5) in the sequence of the grain size of the samples. The sample with intermediate grain sizes (Fe#3) shows the shortest magnetic correlations whereas the magnetic correlations increase with smaller (Fe27, Fe23) as well as with larger (Fe#6, Fe#9) grain sizes.

Fig. 5 summarizes the SANS results for all Fe samples by presenting the (volume-weighted) average magnetic correlations  $L_{\text{mag}} = \langle L^4 \rangle / \langle L^3 \rangle$  as a function of the average grain size  $D$ . The general trend in Fig. 5 is a continuous decrease of  $L_{\text{mag}}$  with decreasing grain size down to a size of about 35 nm, and an increase as the grain size decreases further.

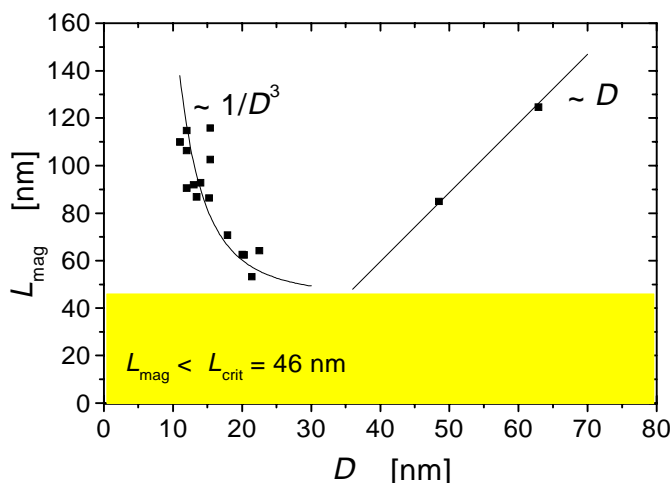


**Figure 5**

Average spatial magnetic correlation length  $L_{\text{mag}}$  versus average grain size  $D$ , for nanostructured Fe. The solid line in the low grain size regime is primarily a guide for the eye, but also represents a fit proportional to  $1/D^3$  predicted by the random-anisotropy model (RAM). No magnetic correlations with  $L_{\text{mag}} < L_{\text{crit}}$  are found (gray shadowed region). Samples with  $D > 80$  nm, leading to  $L_{\text{mag}} > 150$  nm, are not shown in the figure (cf. text).

## 5. Discussion

For grain sizes below  $D = 35$  nm in Fe, the experimental results yield an increasing correlation length with decreasing grain size (cf. Fig. 5). This gives evidence that several grains are magnetically correlated and that these correlations combine progressively more grains when the grain size is further decreased; for  $D = 10$  nm about  $10^3$  grains are magnetically correlated, while for  $D = 60$  nm only about  $2^3$  are correlated.

A basic mechanism leading to a finite correlation length in alloys with uniform exchange but randomly varying anisotropy has been proposed by Alben *et al.* (1978). Within this so-called random-anisotropy model (RAM) the magnetization adjusts to the statistical fluctuations of the anisotropy beyond a finite subvolume of size  $V$  (containing  $N$  particles). Since, within the subvolume  $V$ , exchange between the particles prevents the adjustment of the magnetization to the randomly varying anisotropy, the competition between exchange energy and anisotropy energy results in a finite correlation length  $L_{\text{mag}}$ . More precisely, the effective anisotropy energy in the subvolume  $V$  is reduced by averaging the anisotropy energies of the magnetically coupled grains, *i.e.*  $E_r \sim -KV/\sqrt{N}$ , with  $N = (L_{\text{mag}}/D)^3$  and  $K$  the anisotropy constant. With the exchange energy,  $E_{\text{ex}} \sim AV/L_{\text{mag}}^2$  ( $A$  = exchange constant), the minimization of  $(E_{\text{ex}} + E_r)$  gives  $L_{\text{mag}} \sim (A/K)^{2/3}/D^3$ . This equation is (except for a different exchange constant) also valid for a reduced exchange coupling between the grains (Löffler *et al.*, 1999). Indeed, the SANS data in the low grain size regime follow a function  $L_{\text{mag}} \sim 1/D^3$ , cf.

Fig. 5. Thus, the SANS results give evidence that the magnetic properties of nanostructured materials with low grain sizes are determined by the competition between exchange and anisotropy.

Above a certain size scale, when the grain size exceeds the domain-wall width, domains can form within one grain. This situation can no longer be reconciled with the RAM. Indeed, we find experimentally that above 35 nm the magnetic correlation length increases again in Fe (cf. Fig. 5), giving evidence for a crossover of the magnetic properties at this size scale. The crossover at 35 nm is very close to the effective bulk domain-wall width in Fe,  $L_{\text{crit}} = \pi\delta = 46$  nm, with  $\delta = \sqrt{A/K}$  ( $K = 4.7 \times 10^5$  erg/cm<sup>3</sup>,  $A = 10^{-6}$  erg/cm). Thus, above this size, the increase of  $L_{\text{mag}}$ , which approximately follows the increase in grain size, can be attributed to single-domain grains.

Furthermore, we do not find magnetic correlations  $L_{\text{mag}}$  which are smaller than  $L_{\text{crit}} = 46$  nm (gray shadowed region in Fig. 5). This is in accordance with theoretical studies (Braun, 1999; Löffler *et al.*, 1999), which predict that *nonuniform* magnetization configurations can only exist in grains with sizes larger than  $L_{\text{crit}} = \pi\delta$ . Comparing the results of Fe with those of Co and Ni (Fig. 2), one realizes that in Co the smallest correlation lengths [down to around 20 nm ( $= 2\pi/0.3$  nm<sup>-1</sup>)] are found. In contrast, the magnetic correlation lengths are largest, *i.e.* above 100 nm, in Ni. These values are in reasonable agreement with the length scales  $L_{\text{crit}}$  which are 16 nm for hcp Co and 120 nm for Ni, using the bulk values for  $A$  and  $K$ .

In the validity range of the RAM, the minimum energy is proportional to  $(K^4 V / A^3) D^6$ . Assuming that this minimum energy is equal to  $M_s H_c V$  (where  $M_s$  is the saturation magnetization), a coercive field of the form  $H_c \sim (K^4 / (A^3 M_s)) D^6$  can be estimated. Magnetization measurements have shown that the coercive field of many nanostructured compounds obeys a  $D^6$  scaling law for small grain sizes followed by a decrease for larger grains (Herzer, 1992). Likewise, magnetization measurements on nanostructured Fe show

that the coercive field has a maximum at grain sizes of around 35 nm (Löffler *et al.*, 1998). This is in accordance with the SANS results, which confirm the theoretical predictions of the RAM by *direct* investigation of the intergranular magnetic correlations and their grain size dependence.

## 6. Conclusions

We have presented a SANS study on magnetic correlation lengths in nanostructured Fe, Co and Ni. We found that the spontaneous spatial magnetic correlations forming in zero-field extend over many individual grains. The correlation length strongly depends on grain size and exhibits a minimum, which for Fe lies in the range of 35 nm. For grain sizes below this length scale the correlation length sharply increases.

The increase in the low grain size regime can be explained on the basis of the random-anisotropy model, considering that the effective anisotropy constant results from a statistical average of the anisotropies of magnetically coupled grains. Above a certain size, however, where domain walls can form within one grain, the magnetization direction can change from grain to grain to accommodate to the anisotropy direction of the individual grains. In this case, the grains behave like single-domain particles and the magnetic correlation length follows approximately the increase in grain size.

We further find that, in Fe, the crossover of the magnetic correlation length occurs at grain sizes of around 35 nm, comparable with the effective bulk domain-wall width  $L_{\text{crit}} = \pi \delta = 46$  nm. This crossover was also found by magnetization measurements on nanostructured Fe showing a maximum of the coercive field at a grain size of about 35 nm. Furthermore, in accordance with other experimental and theoretical investigations, we do not find magnetic correlations  $L_{\text{mag}}$  smaller than  $L_{\text{crit}}$ . The latter is also reflected by measurements on Co and Ni. In accordance with the critical length scales of Co and Ni, the SANS results show magnetic correlations down to 20 nm in Co and down to only 100 nm in Ni.

The SANS experiments were performed in collaboration with A. Wiedenmann (HMI Berlin). The authors acknowledge stimulating discussions with H. B. Braun (PSI Villigen) and A. Wiedenmann. The work was supported by the Swiss National Science Foundation and by the Alexander von Humboldt Foundation via the Feodor Lynen Program (J.L.).

## References

- Alben, R., Becker, J. J. & Chi, M. C. (1978). *J. Appl. Phys.*, **49**, 1653 – 1658.
- Braun, H. B. (1999). *J. Appl. Phys.*, **85**, 6172 – 6174.
- Gleiter, H. (1989). *Prog. Mater. Sci.*, **33**, 223 – 315.
- Haas, V. & Birringer, R. (1992). *Nanostruct. Mat.*, **1**, 491 – 504.
- Herzer, G. (1992). *J. Magn. Magn. Mater.*, **112**, 258 – 262.
- Klug, H. P. & Alexander, L. E. (1974). *X-ray Diffraction Procedures for Polycrystalline and Amorphous Materials*, 2nd ed., pp. 661 – 665. New York: Wiley.
- Kostorz, G. (1979). *Treatise on Materials Science and Technology*, Vol. 15: Neutron Scattering, edited by G. Kostorz, pp. 239 – 240. New York: Academic Press.
- Löffler, J., Wagner, W., Van Swygenhoven, H. & Wiedenmann, A. (1997). *Nanostruct. Mat.*, **9**, 331 – 334.
- Löffler, J. F., Meier, J. P., Doudin, B., Ansermet, J.-Ph. & Wagner, W. (1998). *Phys. Rev. B*, **57**, 2915 – 2924.
- Löffler, J. F., Braun, H. B. & Wagner, W. (1999). *J. Appl. Phys.*, **85**, 5187 – 5189.
- Shull, C. G. & Wilkinson, M. K. (1955). *Phys. Rev.*, **97**, 304 – 310.
- Wagner, W., Wiedenmann, A., Petry, W., Geibel, A. & Gleiter, H. (1991). *J. Mater. Res.*, **6**, 2305 – 2311.
- Wagner, W., Van Swygenhoven, H., Höfler, H. J. & Wiedenmann, A. (1995). *Nanostruct. Mat.*, **6**, 929 – 932.
- Weissmüller, J., McMichael, R. D., Barker, J., Brown, H. J., Erb, U. & Shull, R. D. (1997). *MRS Symp. Proc.*, **457**, 231 – 236.
- Yoshizawa, Y., Oguma, S. & Yamauchi, K. (1988). *J. Appl. Phys.*, **64**, 6044 – 6047.